J. Fluid Mech. (1988), *vol.* 187, *pp.* 395–407
Printed in Great Britain

Free-surface effects on spin-up

By ULF CEDERLÖF

Department of Oceanography, University of Gothenburg, Box 4038,
400 40 Gothenburg, Sweden

(Received 26 November 1979 and in revised form 30 July 1987)

The effects of a free surface on the spin-up of a homogeneous fluid are studied, both analytically and experimentally. The analysis is carried out in cylindrical geometry and shows that the spin-up process is strongly modified as the rotational Froude number $F = 4\Omega^2 L^2/gH$ becomes large. The dynamic effect of the free surface causes delayed response outside a sidewall boundary layer of thickness $LF^{-\frac{1}{2}}$. The timescale in the slowly decaying core is larger than the usual spin-up time by a factor of order F. A set of laboratory experiments using a cylinder with a parabolic bottom were carried out in order to test the theory. Reasonable agreement is found in all the experiments except close to the centre where an interesting deviation was observed, especially in cases corresponding to smaller Froude numbers. The deviation consisted of an anticyclonic vortex at the centre. It is shown that this phenomenon might be explained by Lagrangian mean motion resulting from inertial oscillations. In fact, the analysis shows that this motion produces a singular vortex at the centre.

1. Introduction

Greenspan & Howard (1963) gave an extensive analysis of homogeneous spin-up in containers of arbitrary shape, and the reader is referred to this paper for a thorough discussion of spin-up dynamics. They showed, in particular, that in right-circular geometry, the fluid, away from boundaries, spins up as a solid body, i.e. the zonal velocity is linearly dependent on the radial coordinate. We consider here the modification of this theory due to a free surface.

A very brief discussion of this effect was in fact given by Greenspan & Howard in the above-cited paper. They did not present a detailed analysis of the problem, but merely stated the first-order correction for a small rotational Froude number. In the flat-bottom case they found that, to this order, the fluid still spins up as a solid body. It is shown here that this result involves two counteractive effects:

(i) the geometric effect, caused by the paraboloidal shape of the equilibrium surface. This part remains the same if the surface is covered by a rigid frictionless lid of the same shape and therefore cannot be considered a true free-surface effect;

(ii) the dynamic effect, caused by the flexibility of the surface.

The first-order corrections from each of these two effects depart from solid rotation, but the deviations from solid rotation cancel out, leaving the simple result of Greenspan & Howard. Thus, in this particular geometry, the actual free-surface effect is not indicated by the first-order correction. In order to eliminate the geometric effect, which is of no interest in the present context, we use a paraboloidal bottom. In this way, we are able to keep uniform depth and avoid any restriction on the Froude number. The only depth variation is the one induced by the transition between the initial and final parabolas and this is assumed to be small in a linear

theory. This choice of geometry is interesting also from the geophysical point of view, since the oceans are basically thin fluid layers, parallel to the geopotential surface.

Pedlosky (1967) considered the spin-up of a two-layer fluid in a flat-bottomed cylinder. This case offers an alternative way of eliminating the geometric effect, not discussed in his paper. In fact, there is a formal analogy between the homogeneous and two-layer cases when the following limits are taken simultaneously: (i) inviscid upper layer; (ii) infinite upper-layer thickness; (iii) vanishing rotation rate; and (iv) vanishing density jump. In this case, the equations governing the lower layer are essentially the same as those used for the free-surface case. The formulation used here avoids the disturbing processes involved in the two-layer case and focuses directly on the free-surface effect in a way that is easily realized in the laboratory. Experimental studies of two-layer spin-up have been reported by Berman, Bradford & Lundgren (1978) and Linden & Van Heijst (1984). The former were concerned with the interfacial shape during both steady and step spin-up in a centrifuge. This theory includes a geometric effect and shows the same type of boundary-layer response as discussed here. Measurements were reported only of the central height of the interface however. The latter reference deals with the formation of a bare spot when the central depression of the interface reaches the bottom of the tank. Goller & Ranov (1968) studied spin-up from rest in a cylinder of a homogeneous layer with a free surface. This fully nonlinear case was solved by numerical methods and the results were compared with laboratory measurements of the surface elevation.

A set of laboratory experiments, using a cylinder with paraboloidal bottom were carried out. Instead of monitoring the time development of the surface slope, as done in earlier spin-up experiments (for example Goller & Ranov 1968; Berman *et al.* 1978), we found it easier and more accurate to measure fluid displacement during the process. This was done for a range of Froude numbers and the results are presented in §4. Theory is essentially confirmed by experiments. In the central region, however, a rather unexpected deviation from theory occurred. The deviation is characterized by an anticyclonic vortex at the centre, growing in magnitude as the Froude number decreases. Section 5 is devoted to an investigation of this phenomenon. It is shown, by means of a simple analytical model, that the observed feature might be caused by Lagrangian mean motion from the set of inertial oscillations that are generated by the impulsive change of the rotation rate.

2. Quasi-geostrophic theory

In a cylindrical coordinate system (r, θ, z), rotating about the z-axis with angular frequency Ω, the equations governing axisymmetrical flow away from viscous boundary layers are

$$\frac{\mathrm{d}u}{\mathrm{d}t} - 2\Omega v = \frac{1}{\rho}\frac{\partial p}{\partial r} + \Omega^2 r, \tag{2.1}$$

$$\frac{\mathrm{d}v}{\mathrm{d}t} + 2\Omega u = 0, \tag{2.2}$$

$$\frac{\mathrm{d}w}{\mathrm{d}t} = -\frac{1}{\rho}\frac{p}{\partial z} - g, \tag{2.3}$$

$$\frac{\partial w}{\partial z} + \mathrm{D}u = 0. \tag{2.4}$$

The following abbreviations are used throughout this paper:

$$\mathrm{D} = \frac{1}{r}\frac{\partial}{\partial r}r; \quad \mathrm{D}_0 = \frac{1}{r}\frac{\partial}{\partial r}r\frac{\partial}{\partial r}; \quad \mathrm{D}_1 = \frac{\partial}{\partial r}\frac{1}{r}\frac{\partial}{\partial r}r.$$

The fluid is confined within the region

$$r \leqslant L,$$

$$N(r) \leqslant z \leqslant N(r)+H+\eta(r,t),$$

where $N(r) = \Omega^2 r^2/2g$ denotes the shape of the equilibrium parabola, H is the initially constant depth and $\eta(r,t)$ represents the transient distortion of the free surface. The pressure is consistently expressed by

$$p = \rho g[H+N(r)-z]+\phi(r,z,t).$$

The motion is initiated by an impulsive change, $\Delta\Omega$, of the rotation rate at $t = 0$, and the coordinate system is chosen such that the boundaries are at rest. The velocity scale is then given by $U = \epsilon\Omega L$, where $\epsilon = \Delta\Omega/\Omega$ is the Rossby number. The equations are non-dimensionalized using the following scales:

$$[u,v,w,\phi,\eta] = U\left[E^{\frac{1}{2}}, 1, \delta E^{\frac{1}{2}}, 2\rho\Omega L, \frac{2\Omega L}{g}\right],$$

$$[r,z,t] = [L, H, E^{-\frac{1}{2}}\Omega^{-1}].$$

The scale of η is determined by the difference between the initial and final parabolas. E is the Ekman number, defined by $E = \nu/\Omega H^2$. It is assumed that $E \ll 1$.

In the limit $\epsilon = 0$, (2.1)–(2.4) take the non-dimensional form, correct to $O(E^{\frac{1}{2}})$,

$$v = \frac{\partial\phi}{\partial r}, \tag{2.5}$$

$$\frac{\partial v}{\partial t}+2u = 0, \tag{2.6}$$

$$\frac{\partial\phi}{\partial z} = 0, \tag{2.7}$$

$$\frac{\partial w}{\partial z}+\mathrm{D}u = 0. \tag{2.8}$$

Thus the interior motion is geostrophic and hydrostatic to this order, implying

$$\frac{\partial u}{\partial z} = \frac{\partial v}{\partial z} = 0; \quad \eta = \phi.$$

Conditions on the normal components of the interior velocity are imposed by divergent viscous boundary layers on the bottom and sidewalls. At the bottom, the vertical velocity induced by the Ekman layer is (Greenspan 1969)

$$w_{\mathrm{b}} = \tfrac{1}{2}(1+\alpha^2 r^2)\,\mathrm{D}\frac{\partial\phi}{\partial r}(1+\alpha^2 r^2)^{\frac{1}{4}}, \tag{2.9}$$

where $\alpha = \Omega^2 L/g$ measures the importance of centrifugal force relative to gravitation or the inclination of the equipotential surface. Large values of α introduce effects

outside the scope of the present analysis and we shall assume that $\alpha \ll 1$. With this assumption, the complete bottom condition becomes

$$w_b = \tfrac{1}{2}D_0\phi + u\frac{\partial N}{\partial r}. \tag{2.10}$$

The linearized free-surface condition for the vertical velocity is given by

$$w_s = \tfrac{1}{2}F\frac{\partial \phi}{\partial t} + u\frac{\partial N}{\partial r}, \tag{2.11}$$

where $F = 4\Omega^2 L^2/gH$ is the rotational Froude number.

Vertical integration of the continuity equation (2.8), using (2.5), (2.6), (2.10) and (2.11), yields

$$F\frac{\partial \phi}{\partial t} = D_0\phi + D_0\frac{\partial \phi}{\partial t}. \tag{2.12}$$

The left-hand side of this equation represents the effect of the free surface, and the Froude number is a measure of its magnitude. On the right-hand side are the divergencies of the Ekman and interior fluxes respectively. Equation (2.12) is to be solved subject to the initial condition

$$\phi = -\tfrac{1}{2}(r^2 - \tfrac{1}{2}) \quad \text{at } t = 0. \tag{2.13}$$

The appropriate condition at $r = 1$ is obtained from the requirement of zero net flux through the sidewall:

$$\frac{\partial \phi}{\partial r} + \frac{\partial}{\partial t}\frac{\partial \phi}{\partial r} = 0 \quad \text{at } r = 1. \tag{2.14}$$

At this point we can confirm the statement made in §1 concerning the first-order correction to the constant-depth case from the two effects of a free surface. To include the variation of depth in the flat-bottom case, we have only to multiply the interior mass flux term in (2.12) by the total depth, yielding

$$F\frac{\partial \phi}{\partial t} = D_0\phi + D(1 + \tfrac{1}{8}F(r^2 - 1))\frac{\partial}{\partial r}\frac{\partial \phi}{\partial t},$$

with

$$(1 + \tfrac{1}{8}F(r^2 - 1))\frac{\partial}{\partial r}\frac{\partial \phi}{\partial t} + \frac{\partial \phi}{\partial r} = 0 \quad \text{at } r = 1.$$

If we assume that $F \ll 1$ and introduce the asymptotic expansion

$$\frac{\partial \phi}{\partial r} = v = v^0 + Fv^1 + \ldots,$$

it is found that

$$v^0 = r(1 - e^{-t})$$

and

$$v^1 = \tfrac{1}{16}rt\, e^{-t},$$

which is identical with the result obtained by Greenspan & Howard. On the other hand, if we go through the same procedure with (2.12)–(2:14), we find that

$$v^1 = \tfrac{1}{16}r^2 t\, e^{-t}$$

which is not linear in r.

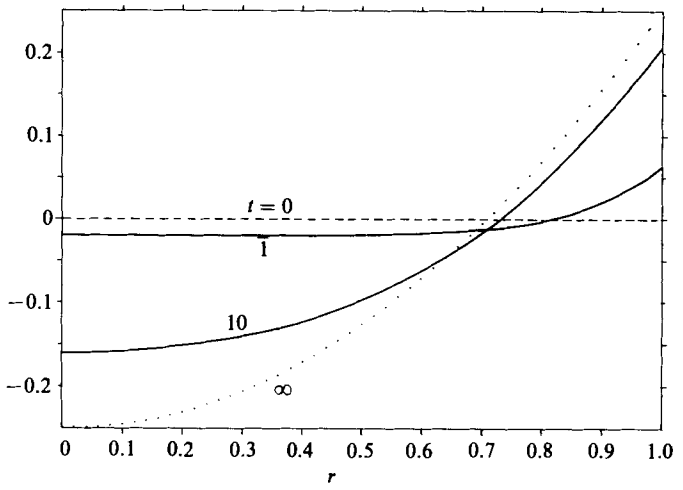

FIGURE 1. Plots of the free-surface shape for three stages of spin-up. Computations are made from (3.2) with $F = 100$.

3. Solution and discussion

The boundary condition (2.14) may be integrated over time yielding

$$\frac{\partial \phi}{\partial r} = -\mathrm{e}^{-t} \quad \text{at } r = 1. \tag{3.1}$$

Thus, close to the wall, the decay time is $O(1)$, which is the usual spin-up timescale obtained with $F = 0$. Inspection of (2.12) shows that for large F, this timescale is characteristic only in a sidewall boundary layer of thickness $F^{-\frac{1}{2}}$, where all three terms of (2.12) are of equal importance. In the main part of the fluid, the timescale is $O(F)$, and here the last term of (2.12) is $O(F^{-1})$, while the other two are $O(1)$, leaving essentially a diffusion equation for the pressure. In other words, there are two very different processes involved when $F \gg 1$, one rapid in the boundary layer and one slow 'diffusive' outside it.

The complete solution of (2.12)–(2.14) is obtained by separation of variables and Fourier–Bessel expansion:

$$\phi = -\tfrac{1}{2}(r^2 - \tfrac{1}{2})\,\mathrm{e}^{-t} + 2 \sum_{k=1}^{\infty} \frac{J_0(\mu_k r)}{\mu_k^2 J_0(\mu_k)} (\mathrm{e}^{S_k t} - \mathrm{e}^{-t}), \tag{3.2}$$

where μ_k is the kth zero of $J_1(r)$ and

$$S_k = -\frac{\mu_k^2}{\mu_k^2 + F}.$$

Some results computed from (3.2) with $F = 100$ are displayed in figures 1 and 2. In figure 1, the surface elevation at a few stages of spin-up is plotted relative to the initial state. It is seen that the early response is confined to a region close to the sidewall. Figure 2 is a simple plot of the decay time versus radial position. Both figures confirm the above discussion.

In view of these results, the spin-up process may be described in the following way. Shortly after the start ($t \sim E^{\frac{1}{2}}$), the boundary-layer circulation is fully developed and

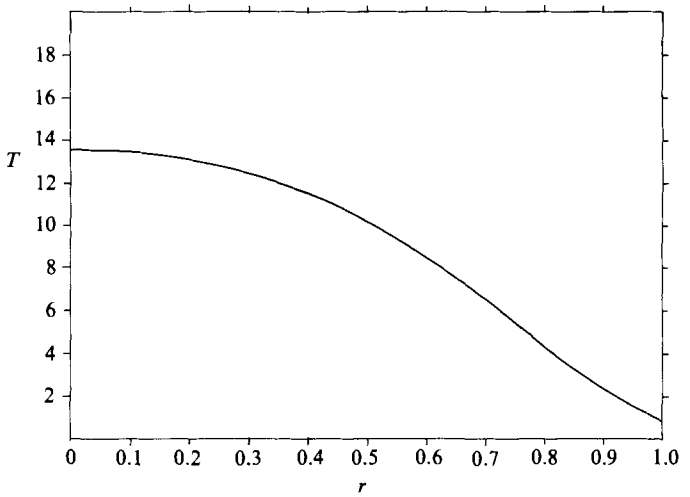

FIGURE 2. Plot of the e-folding time versus radius, computed from (3.2) with $F = 100$.

the radial flow delivered by the thin Stewartson layer acts as a barotropic signal that, within a few revolutions, penetrates (with the speed of a long wave) a distance of the order $F^{-\frac{1}{2}}$ into the fluid, where it is blocked by rotation. Outside this region (the Rossby radius) there is no radial flow in the early stage and the surface simply descends at the Ekman suction rate. The fluid within the layer is zonally accelerated and a velocity gradient is produced in such a way that the vertical Ekman flux changes sign somewhere close to the wall. This point of zero Ekman-layer divergence separates the central region where fluid is withdrawn by Ekman suction from the outer region where it is redelivered. At $t \sim 1$, the width of the outer region is of the order of the external Rossby radius of deformation, growing slowly to cover the whole volume at $t \sim F$. The slow phase is mathematically a diffusion process with a diffusion coefficient equal to F^{-1} (dimensionally $L^2\Omega F^{-1}$). Thus free-surface spin-up at large Froude number requires a longer time and consequently more energy. The excess energy is used to build up the potential energy, stored in the final parabola.

4. Experiments

A set of experiments in a cylinder with a paraboloidal bottom were carried out, in order to confirm the predicted dependence on F. There is a small problem in designing experiments with large external Froude numbers if, in addition, the parameters $\alpha = \Omega^2 L/g$ is to be kept small. The radius of the cylinder used in the experiments was 14.5 cm and the rotation rate was 3.718 rad/s. This gives 0.2 for α, which should allow the curvature to be safely ignored in (2.9). The maximum value, 23.7, of F was obtained with a very thin fluid layer (5 mm). This case represents the limit considered in the theory and is the one showing the closest agreement. The ratio of the widest Stewartson layer to the Rossby radius is of the order $\delta E^{\frac{1}{4}} F^{\frac{1}{2}}$, which is small in all cases. Parameter values for five experiments are given in table 1. These experiments were repeated several times with no significant difference in results.

The angular displacement of fluid during the process was measured by photographic registration of an initially radial dye streak (figure 3). For simplicity,

exp	H/L	$\epsilon \times 10^2$	$E \times 10^4$	F
I	0.034	3.67	108.0	23.7
II	0.069	3.40	27.0	11.8
III	0.138	3.40	6.7	5.9
IV	0.207	3.40	3.0	4.0
V	0.276	3.40	1.7	3.0

TABLE 1. Parameter values for the experiments

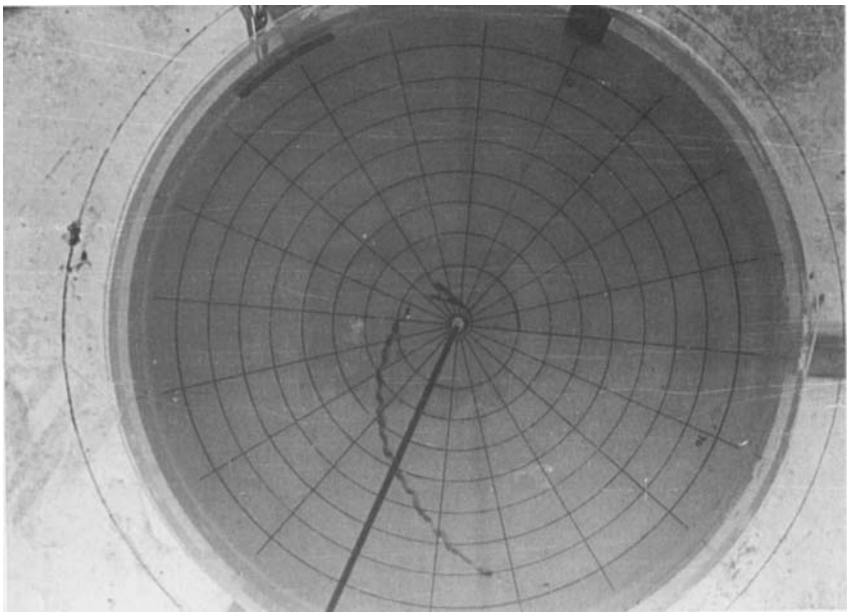

FIGURE 3. Photograph showing the appearance of the dye streak in experiment IV ($F = 4.0$), taken at $t = 180$ s. Note the developing central vortex.

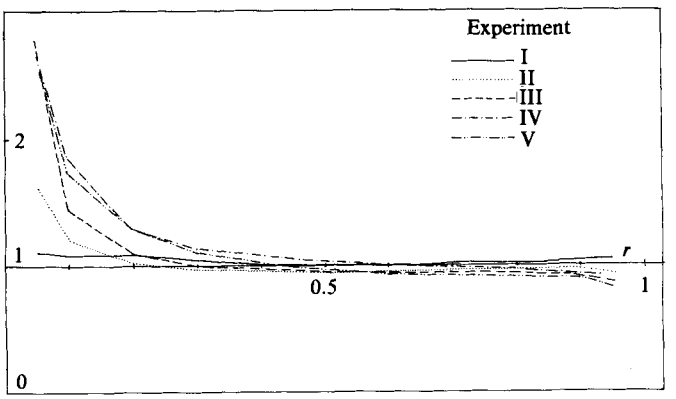

FIGURE 4. Experimental results, presented as total angular displacement versus radius. The data (originally in radians) have been scaled by the factor $\epsilon E^{-\frac{1}{2}}$ and divided by (4.1). Thus, the theoretical prediction coincides with the r-axis.

we consider only the final position of the dye, i.e. the total angular displacement. This quantity is not only easy to measure accurately, but also the theoretical prediction for it can be put into a simple analytical form:

$$\theta = \int_0^\infty \frac{v}{r}\mathrm{d}t = \int_0^\infty \frac{1}{r}\frac{\partial \phi}{\partial r}\mathrm{d}t.$$

Integration of (2.12), using (2.13)–(2.14) yields

$$\theta = \tfrac{1}{8}F(r^2-1)-1. \tag{4.1}$$

This formula shows once again that the timescale varies from 1 at the sidewall to F in the centre. Multiplying (4.1) with the scale factor $\epsilon E^{-\frac{1}{2}}$ gives the actual angular displacement in radians. The experimental results are shown in figure 4, properly scaled and divided by the theoretical expression (4.1). The plots in figure 4 show the general agreement with theory, at least in the region away from the centre and the rim. They also show that a central anticyclonic vortex, growing in magnitude and radius with the aspect ratio, develops. Note that (4.1) also predicts an anticyclonic motion, increasing towards the centre. Thus the observed deviation acts to amplify the curly shape of the dye streak (see figure 3).

5. Inertial oscillations

Initial-value problems in contained rotating flow always involve the generation of inertial oscillations. These oscillations play an important role in the early stage of the interior response. Quasi-geostrophic theory alone cannot support arbitrary initial conditions. In addition to the geostrophic flow, there are two contributions, generally not considered in problems like this. One of these is associated with components of the forcing, having timescales of the order $1/\Omega$. The other consists of an infinite set of inertial oscillations generated by the discontinuity inherent in the initial condition. Such discontinuities always occur when the fluid is subject to sudden changes in the external forcing, like the impulsive change of the rotation rate in the spin-up problem. The imposed initial condition is satisfied by the sum of the three flow components. Unlike the geostrophic and transient components, the inertial oscillations are independent of the forcing except at the discontinuity and thus merely constitute a superimposed decaying motion that eventually disappears.

The general properties of contained inertial oscillations have been studied by many authors and numerous reports have been published. For a comprehensive account, see Greenspan (1969). The objective here is solely to demonstrate that inertial oscillations can produce phenomena qualitatively similar to the disturbances reported in §3. A complete analysis of the initial-value problem including inertial oscillations would be extremely complicated and therefore we shall use a simple model to simulate the generation of oscillations that take place in the spin-up problem. The results from this model show that inertial oscillations give rise to Lagrangian mean motion. In particular, a singular vortex is produced at the centre. This spiral motion is the most spectacular feature found in the experiments. With decreasing aspect ratio, H/L, the mean circulation from oscillations gets confined to narrowing regions at the centre and rim. This could explain why experiments corresponding to small aspect ratios show little or no deviation from quasi-geostrophic theory.

In order to simulate the generation of inertial oscillations in the simplest possible

way, yet relevant to the present problem, we shall use cylindrical geometry with a flat top and bottom. We have thereby assumed that the paraboloidal shape, used in the previous sections, is not the primary cause of the phenomenon we are looking for. In quasi-geostrophic theory, variations of the rotation rate are transmitted to the interior via Ekman layers at the horizontal surfaces. The effect on the interior is a horizontally homogeneous vertical flux with return flow in the corner region. The strength of the flux is determined by the velocity difference between the geostrophic flow and the horizontal boundary. In the present model, we shall simply impose an artificial Ekman flux with given time-dependent amplitude and solve the following linearized inviscid problem:

$$\frac{\partial u}{\partial t} - 2\Omega v = -\frac{1}{\rho}\frac{\partial \phi}{\partial r}, \tag{5.1}$$

$$\frac{\partial v}{\partial t} + 2\Omega u = 0, \tag{5.2}$$

$$\frac{\partial w}{\partial t} = -\frac{1}{\rho}\frac{\partial \phi}{\partial z}, \tag{5.3}$$

$$\frac{\partial w}{\partial z} + \mathrm{D}u = 0, \tag{5.4}$$

with boundary conditions

$$w = F(t)\, w_0; \quad z = 0, \tag{5.5}$$

$$w = G(t)\, w_0; \quad z = H, \tag{5.6}$$

$$u = 0; \qquad r = 0, L, \tag{5.7}$$

$$u, v, w = 0; \qquad t \leqslant 0. \tag{5.8}$$

The system is non-dimensionalized according to ($\delta = H/L$)

$$[u, v, w, \phi] = W_0[\delta^{-1}, \delta^{-1}, 1, 2\rho L\Omega\delta^{-1}],$$

$$[r, z, t] = \left[L, H, \frac{1}{2\Omega}\right]$$

and thus takes the form

$$\frac{\partial u}{\partial t} - v = -\frac{\partial \phi}{\partial r}, \tag{5.9}$$

$$\frac{\partial v}{\partial t} + u = 0, \tag{5.10}$$

$$\delta^2 \frac{\partial w}{\partial t} = -\frac{\partial \phi}{\partial z}, \tag{5.11}$$

$$\frac{\partial w}{\partial z} + \mathrm{D}u = 0. \tag{5.12}$$

We introduce a meridional stream function ψ according to

$$u = \frac{\partial \psi}{\partial z}; \quad w = -\mathrm{D}\psi. \tag{5.13}$$

Elimination of v and ϕ gives the following problem for the stream function:

$$\delta^2 \mathrm{D}_1 \frac{\partial^2 \psi}{\partial t^2} + \left(\frac{\partial^2}{\partial t^2} + 1\right) \frac{\partial^2 \psi}{\partial z^2} = 0, \tag{5.14}$$

with boundary and initial conditions

$$\begin{aligned} \psi &= 0; && r = 0, 1, \\ \psi &= -\tfrac{1}{2} r F(t); && z = 0, \\ \psi &= -\tfrac{1}{2} r G(t); && z = 1, \\ \psi &= 0; && t \leqslant 0. \end{aligned}$$

Taking the Laplace transform of (5.14) yields

$$\delta^2 s^2 \mathrm{D}_1 \tilde{\psi} + (s^2 + 1) \frac{\partial^2 \tilde{\psi}}{\partial z^2} = 0, \tag{5.15}$$

with

$$\left.\begin{aligned} \tilde{\psi} &= 0; && r = 0, 1, \\ \tilde{\psi} &= -\tfrac{1}{2} r \tilde{F}(s); && z = 0, \\ \tilde{\psi} &= -\tfrac{1}{2} r \tilde{G}(s); && z = 1. \end{aligned}\right\} \tag{5.16}$$

The transformed stream function is expanded in a Fourier–Bessel series:

$$\tilde{\psi} = \sum_{k=1}^{\infty} \tilde{a}_k(z) J_1(\mu_k r). \tag{5.17}$$

Insertion of (5.17) into (5.15) gives the following equation for the Fourier–Bessel coefficients:

$$\frac{\partial^2 \tilde{a}_k}{\partial z^2} - \mathscr{H}_k^2 \tilde{a}_k = 0, \tag{5.18}$$

where

$$\mathscr{H}_k^2 = \frac{\delta^2 \mu_k^2 s^2}{1 + s^2}. \tag{5.19}$$

The solution of (5.18) using (5.16) is

$$\tilde{a}_k(z) = -\tfrac{1}{2} \xi_k \frac{\tilde{G}(s) \sinh \mathscr{H}_k z + \tilde{F}(s) \sinh \mathscr{H}_k (1 - z)}{\sinh \mathscr{H}_k}, \tag{5.20}$$

where

$$\xi_k = -\frac{2}{\mu_k J_0(\mu_k)}.$$

The analysis so far applies to arbitrary time dependence of the forcing. The functions G and F should be chosen to model the spin-up Ekman layer as closely as possible. This is conveniently done by taking the Laplace transformed solution of the classical time-dependent Ekman-layer problem on a rotating disk (Greenspan 1969). With a free surface, G and F are then given by

$$\tilde{G} \equiv 0; \quad \tilde{F} = \frac{\mathrm{i}}{s}[(s + \mathrm{i})^{-\frac{1}{2}} - (s - \mathrm{i})^{-\frac{1}{2}}], \tag{5.21}$$

yielding for $\tilde{a}_k$

$$\tilde{a}_k(z) = -\frac{\mathrm{i}\xi_k}{2s}\left[(s+\mathrm{i})^{-\frac{1}{2}} - (s-\mathrm{i})^{-\frac{1}{2}}\right]\frac{\sinh \mathscr{H}_k(1-z)}{\sinh \mathscr{H}_k}. \tag{5.22}$$

The inversion of $\tilde{a}_k(z)$ is a standard procedure involving the calculation of residues. From the structure of (5.22) it is seen that there are three contributions to the solution. These are

(i) The geostrophic part, corresponding to the simple pole at $s = 0$.

$$-\tfrac{1}{2}\xi_k \sqrt{2}(1-z). \tag{5.23}$$

(ii) The transient part, corresponding to the branch points at $s = \pm\mathrm{i}$.

$$-\frac{\xi_k}{\pi}\,\mathrm{Im}\left\{\int_0^\infty \frac{\mathrm{e}^{(\mathrm{i}-\eta)t}}{(\mathrm{i}-\eta)\,\eta^{\frac{1}{2}}}\frac{\sinh \mathscr{H}_k^+(1-z)}{\sinh \mathscr{H}_k^+}\,\mathrm{d}\eta\right\}, \tag{5.24}$$

where $$\mathscr{H}_k^+ = \mathscr{H}_k(s = \mathrm{i}-\eta).$$

This part constitutes the response to the decaying oscillations at the rotation frequency, typical of the time-dependent Ekman layer.

(iii) The inertial oscillations, corresponding to the simple poles at

$$s = \pm\mathrm{i}\omega_{n,k}; \quad \omega_{n,k} = \left[\frac{(n\pi)^2}{(n\pi)^2 + \delta^2\mu_k^2}\right]^{\frac{1}{2}}.$$

This part is given by

$$\sin n\pi z(\tau\,\mathrm{e}^{\mathrm{i}\omega t} + \tau^*\,\mathrm{e}^{-\mathrm{i}\omega t}), \tag{5.25}$$

where $$\tau = \tau_0(A+\mathrm{i}B); \quad \tau_0 = \tfrac{1}{2}\xi_k\frac{\sqrt{2}}{n\pi}(1-\omega^2)^{\frac{1}{2}};$$

$$A = \tfrac{1}{2}[(1-\omega)^{\frac{1}{2}} + (1+\omega)^{\frac{1}{2}}],$$

$$B = \tfrac{1}{2}[(1-\omega)^{\frac{1}{2}} - (1+\omega)^{\frac{1}{2}}].$$

The sum of (5.23)–(5.25) constitutes the complete solution. From here on, we shall focus attention on the last part and calculate the Lagrangian mean motion resulting from the inertial oscillations. This phenomenon, which is generally associated with progressive gravity waves (Stokes drift), is due to the fact that individual fluid particles in oscillatory motion travel over finite distances and are therefore influenced by spatial variations of the velocity field. As a consequence, the fluid particles do not necessarily have to follow closed orbits. If not, there is a Lagrangian mean motion which could be detected only by Lagrangian measurements, like following dyed fluid. The Lagrangian zonal velocity is given by

$$v_{\mathrm{L}} = \int_0^t u\mathrm{D}v\,\mathrm{d}t' + \int_0^t w\frac{\partial v}{\partial z}\mathrm{d}t'. \tag{5.26}$$

If the Eulerian velocity components

$$u_{n,k} = -\xi_k\, n\pi J_1(\mu_k r)\cos n\pi z\,\mathrm{Re}\{\tau_{n,k}\,\mathrm{e}^{\mathrm{i}\omega t}\}, \tag{5.27}$$

$$v_{n,k} = \frac{\xi_k}{\omega}\, n\pi J_1(\mu_k r)\cos n\pi z\,\mathrm{Im}\{\tau_{n,k}\,\mathrm{e}^{\mathrm{i}\omega t}\}, \tag{5.28}$$

$$w_{n,k} = \xi_k\,\mu_k J_0(\mu_k r)\sin n\pi z\,\mathrm{Re}\{\tau_{n,k}\,\mathrm{e}^{\mathrm{i}\omega t}\} \tag{5.29}$$

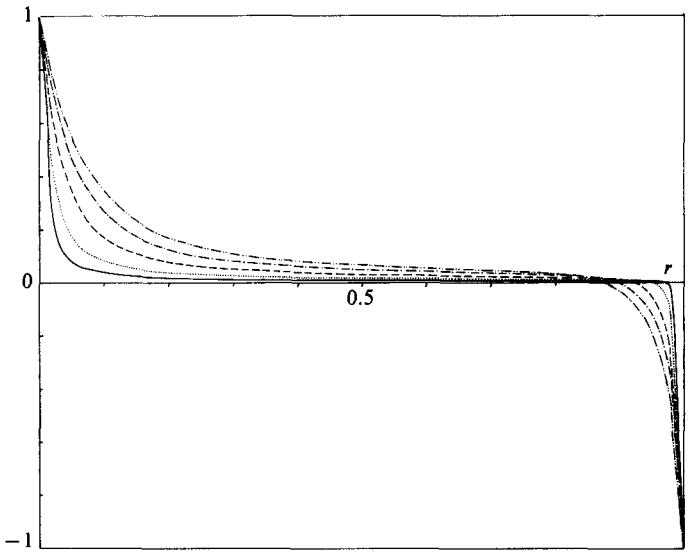

FIGURE 5. Plots of the time-integrated Lagrangian mean motion versus radius, resulting from inertial oscillations. The computations are made from (5.32), using aspect ratios corresponding to the experiments. The curves are normalized by the factor $1/3Er$.

are inserted in (5.26) and the time average is taken, we get

$$\bar{V}_{\mathrm{L}} = -4\frac{1-\omega^2}{\mu_k\omega^2}\frac{J_1(\mu_k r)J_0(\mu_k r)}{J_0^2(\mu_k)}. \tag{5.30}$$

Thus, the Lagrangian mean zonal flow is independent of the vertical coordinate. In order to calculate the total zonal displacement of fluid, decay factors have to be included in the exponents in (5.27)–(5.29). For simplicity, we take the approximate decay factors due to internal friction (ignoring frictional effects from the boundaries)

$$\sigma_{n,k} = \tfrac{1}{2}E((n\pi)^2+\delta^2\mu_k^2). \tag{5.31}$$

Integration of (5.30) yields

$$S_{n,k} = \int_0^\infty \bar{V}_{\mathrm{L}}\,\mathrm{e}^{-\sigma t}\,\mathrm{d}t = -\frac{8}{E}\frac{1-\omega^2}{\mu_k^2(n\pi)^2}\frac{J_1(\mu_k r)J_0(\mu_k r)}{J_0^2(\mu_k)}. \tag{5.32}$$

Investigation of (5.32) in the limits $r\to 0$ and $r\to 1$ shows that

$$S = \sum_{k=1}^{\infty}\sum_{n=1}^{\infty} S_{n,k} \to \frac{1}{3Er} \quad \text{as } r\to 0,$$

$$S = \sum_{k=1}^{\infty}\sum_{n=1}^{\infty} S_{n,k} \to \frac{1}{3E} \quad \text{as } r\to 1.$$

Thus S is singular at $r = 0$. Figure 5 shows plots, computed from (5.32), for aspect ratios corresponding to the five reported experiments (note the qualitative similarity with figure 4). Although the magnitude of S is small (the scale factor is $\epsilon^2E^{\frac{1}{2}}$), the existence of a singularity may still give rise to noticeable circulation at finite distance from the centre. This aspect of inertial oscillations has not (to our knowledge) been reported in the literature and we plan to run a special experimental study of the

problem. In addition to the dynamics discussed in this section, there might be effects from the paraboloidal shape. Woods (1977) for example, showed that radial focusing of inertial oscillations may occur in certain geometries with the result that small-scale modes get strongly amplified in the neighbourhood of the rotation axis. Little is known, however, about the inertial spectrum in geometries other than the cylinder and the sphere.

The author gratefully acknowledges the help and encouragement he received from Professor Gösta Walin.

REFERENCES

BERMAN, A. S., BRADFORD, J. & LUNDGREN, T. S. 1978 Two-fluid spin-up in a centrifuge. *J. Fluid Mech.* **84**, 411–431.

GOLLER, H. & RANOV, T. 1968 Unsteady rotating flow in a cylinder with a free surface. *Trans. ASME* D: *J. Basic Engng* **90**, 445–454.

GREENSPAN, H. P. 1969 *The Theory of Rotating Fluids*. Cambridge University Press.

GREENSPAN, H. P. & HOWARD, L. N. 1963 On a time-dependent motion of a rotating fluid. *J. Fluid Mech.* **17**, 385–404.

LINDEN, P. F. & VAN HEIJST, G. J. F. 1984 Two-layer spin-up and frontogenesis. *J. Fluid Mech.* **143**, 69–94.

PEDLOSKY, J. 1967 The spin-up of a stratified fluid. *J. Fluid Mech.* **28**, 463–479.

WOOD, W. W. 1977 Inertial oscillations in a rigid axisymmetric container. *Proc. R. Soc. Lond.* A **358**, 17–30.